First-principles calculation of 0^{th}-layer graphene-like growth of C on SiC(0001)

Masato Inoue,[1,2,*] Hiroyuki Kageshima,[1] Yoshihiro Kangawa,[2,3] and Koichi Kakimoto[2,3]
[1]*NTT Basic Research Laboratories, NTT Corporation, Atsugi, Kanagawa 243-0198, Japan*
[2]*Department of Aeronautics and Astronautics, Kyushu University, Fukuoka, Fukuoka 819-0395, Japan*
[3]*Research Institute for Applied Mechanics, Kyushu University, Kasuga, Fukuoka 816-8580, Japan*
(Received 10 May 2012; revised manuscript received 13 July 2012; published 8 August 2012)

We use a first-principles approach to analyze the clustering of C atoms during the initial stage of 0^{th}-layer graphene-like growth on SiC(0001). We started the layer with the lowest-energy hexagonal C ring and then let it grow. The growth produced pentagonal rings with a heptagonal ring in a graphene-like (penta-heptagonal) structure. We also studied the chemical potential of C atoms on SiC(0001) and revealed that the C clustering begins at a surface coverage of 0.25–0.33 atom/SiC(0001)-(1×1). Finally, we confirmed that the energetic stabilities of penta-heptagonal clusters on SiC(0001) exceed that of single C rings (7–18 atoms), the lowest-energy structure of free-standing C_{7-18} clusters. Hence, the results show that SiC(0001) acts as a template for graphene-like growth.

DOI: 10.1103/PhysRevB.86.085417 PACS number(s): 68.65.−k, 82.20.Wt, 81.05.−t

I. INTRODUCTION

Graphene, a two-dimensional (2D) sheet of C atoms in a honeycomb pattern, shows promise in future electronic devices, but to build practical graphene-based devices, we need a reliable graphene growth technique. A promising industrial-scale growth technique involves the thermal decomposition of SiC(0001). This method is promising because it may produce epitaxial graphene over the entire SiC substrate.[1] However, graphene with a large domain area and a well-controlled layer thickness on atomically flat SiC(0001) has not yet been achieved due to insufficient understanding of the growth mechanism.[2–4]

Several experimental studies have reported graphene growth on SiC(0001).[5–7] However, experimental difficulties have prevented clarification of the growth process of 0^{th}-layer graphene. This graphene is the first graphene layer grown on bulk-truncated SiC(0001), a layer that constructs the SiC(0001)-$(6\sqrt{3} \times 6\sqrt{3})$R30° superlattice structure and acts as a buffer layer between graphene and SiC(0001).[1] Understanding the growth mechanism of 0^{th}-layer graphene is an important challenge because improvement of its surface morphology is crucial for controlling graphene thickness.[8]

The growth process of 0^{th}-layer graphene involves three elementary processes: (1) thermal decomposition of SiC(0001) leading to Si desorption and C migration, (2) nucleation by C-atom clustering, and (3) lateral growth of the cluster. Clarification of the nucleation process (2) is crucial for understanding 0^{th}-layer graphene growth; moreover, controlling the nucleation rate experimentally is essential for reducing domain boundaries. It has been known that a very initial stage of C-atom clustering (C_{1-3}) exhibits dimers and trimers, while further growth of these small clusters is not clarified.[9] Therefore, in this theoretical study, we focus on the C-atom clustering and the initial lateral growth on SiC(0001) up to C_{20}.

II. COMPUTATIONAL METHOD

Carbon clustering involves C migration, which is influenced by the C supply source and the diffusion length.[10] However, recent techniques have produced graphene growth under quasi-thermal equilibrium. In this case, migrating C atoms are not limited by the diffusion length; rather, they are incorporated into 0^{th}-layer graphene so as to be the most energetically stable.[11,12] Therefore, we ignore here the diffusion length and focus on the C-atom clustering and lateral growth via static energetics. The energetics method is a first-principles pseudopotential calculation scheme. The calculations are based on density functional theory and done using the exchange-correlation functional of generalized gradient approximation (GGA-)PBE96,[13] ultrasoft pseudopotentials, single k-point sampling, and a plane-wave basis set with cutoff energy of 275.5 eV. To simulate isolated C clustering on SiC(0001), we used a SiC(0001)-$(2\sqrt{3} \times 2\sqrt{3})$R30° lateral unit cell with repeated slab geometry (Fig. 1). This large lateral unit cell was chosen to avoid the interaction between C clusters and its replicas. The slab consists of two SiC bilayers; the bottom surface is passivated with hydrogen atoms and a sufficiently thick vacuum region.

Our procedure followed three steps. (1) In step 1, we put on the surface the hexagonal C cluster with the lowest formation energy. (2) We added C atoms one-by-one to various sites around the C cluster and optimized the atomic structure while fixing the bottom SiC bilayer. (3) We determined the most stable structure of the C cluster up to C_{20} by calculating the formation energies E_{form}. The formation energies in this study were calculated by assuming that the surface system is in thermal equilibrium with bare SiC(0001) and isolated graphene. Specifically, $E_{\mathrm{form}} = (E_{\mathrm{total}} - E_{\mathrm{bare}} - N_{\mathrm{C}}\mu_{\mathrm{grn}})/N_{\mathrm{C}}$, where E_{total} is the total energy of the C-adsorbed surface system, E_{bare} is the total energy of the initial surface system, N_{C} is the number of C adatoms, and μ_{grn} is the chemical potential of a C atom in isolated graphene. Then, the energetic stability of C monomers on SiC(0001) was analyzed to investigate the relation between the growth of the C cluster and the environmental conditions. Finally, we compared the structural evolution of C clusters on SiC(0001) with that of free-standing C clusters.

We first evaluated our calculation model by comparing the formation energy of a C-adsorbed SiC(0001)-$(\sqrt{3} \times \sqrt{3})$R30° structure with that from a previous study.[9] Our value of 0.97 eV/atom is close to the previously determined value of

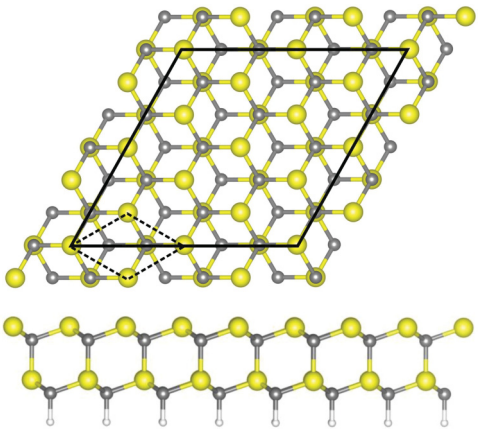

FIG. 1. (Color online) Calculated SiC surface system. The region enclosed by solid lines is the unit supercell of the periodical system SiC(0001)-($2\sqrt{3} \times 2\sqrt{3}$)R30°. The SiC(0001)-($1 \times 1$) cell is shown by dashed lines. Yellow (light gray) spheres are Si atoms, and grey spheres are C. The white spheres on the bottom, bulk-SiC side are H. The C clustering occurs on the top, the Si-terminated surface.

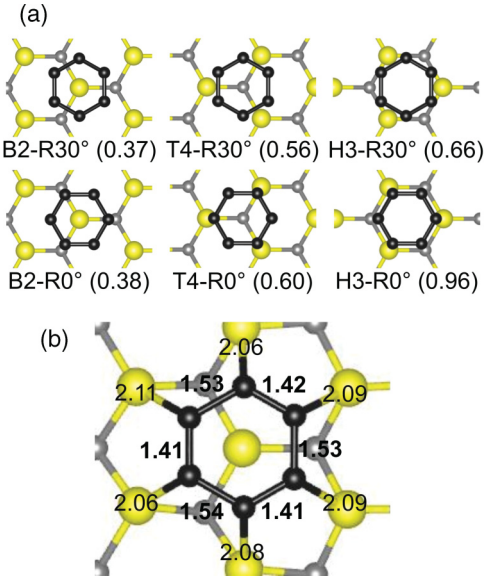

FIG. 2. (Color online) Initial hexagonal C-ring clusters on SiC(0001). (a) The initial configurations of C hexagonal clusters and their formation energies after atomic optimization. Black spheres are C atoms in clusters. Numbers in parentheses are the formation energies (electron volt per atom). (b) The most stable atomic configuration of a C hexagonal cluster. The thick numbers are C-C bond lengths in the cluster (Å). The thin numbers are Si-C bond lengths between the cluster and SiC(0001) (Å).

0.82 eV/atom. In addition, we checked the suitability of using the hexagonal C cluster as the initial condition by tracing the decomposition process. We removed C atoms form the most stable configuration of a hexagonal C cluster (discussed later) one-by-one. We found that the atomic configurations (both structures and locations) of C_3 and C_4 were the same as that in a previous study in which monatomic C decomposed on SiC(0001),[9] and C atoms stabilize by forming a hexagonal cluster. In addition, the hexagonal cluster has a lower formation energy than the C_6 linear cluster, which is the ground-state configuration of a free-standing C_6 cluster. For these reasons, we used the lowest-energy hexagonal cluster as the initial condition.

III. RESULTS AND DISCUSSION

A. C-clustering process on SiC(0001)

For the initial hexagonal cluster, we choose among six initial configurations. As shown in Fig. 2(a), the most energetically preferable configuration is that of B2-R30°, which corresponds to a threefold rotational symmetry point of the ($6\sqrt{3} \times 6\sqrt{3}$)R30° structure.[1] (The B2-R0° configuration has almost the same formation energy as B2-R30° because a hexagonal cluster of B2-R0° rotates by 30° during the atomic structure optimization.) As shown in Fig. 2(b), the B2-R30° (and B2-R0°) cluster retained its initial hexagonal structure upon forming chemical bonds between all C atoms in the cluster and Si atoms on SiC(0001). Other configurations did not; that is, they do not form six chemical bonds with SiC(0001). These Si-C bonds to SiC(0001) affected the lowest energy configuration. It has been known that the free-standing C_6 cluster has a threefold rotational symmetry (D_{3h}) with bonding lengths of 1.32 Å and bonding angles of 93° and 147°.[14] C-C bond lengths of the B2-R30° cluster are longer than those of the free-standing C_6 cluster by 7–17%, indicating tensile strain [Fig. 2(b)]. Other configurations did not exhibit such a large strain. Hence, the energetic stability of B2-R30° can be attributed to the bonds with SiC(0001), which do not cause crucial disorders in the C cluster but aid to keep its hexagonal shape.

We next put C atoms around the stable hexagonal cluster one-by-one to understand the growth process. Figure 3 shows the structural evolution of C clusters C_{7-20}. The result shows that the clusters form penta-heptagonal structures, although unlike the hexagonal rings in graphene, one ring here is a heptagon with the rest being pentagons. The formation energy of these clusters remained around 0.37 eV/atom [(Fig. 4(c)].

To ascertain the preference of C clusters on SiC(0001) for the penta-heptagonal structure, we examined the energetic stability of several purely hexagonal structures shown in Fig. 4(a). These purely hexagonal structures were obtained by adding hexagons to the most stable configuration of the C hexagonal cluster, the B2-R30°. Figure 4(c) shows the formation energy of the lowest-energy configuration of C purely hexagonal clusters. The energy of the clusters with mostly nonhexagons is 0.1–0.3 eV lower than that of purely hexagonal of the same size. This result suggests that penta-heptagonal clusters certainly appear during the clustering process.

During further growth of the penta-heptagonal cluster, the pentagons and heptagons may follow two probable courses. In one, the pentagons and heptagons are excluded from the inside of C cluster but survive at the edge. After all, free-standing graphene expresses some kinds of edge-reconstruction that contains pentagons and heptagons.[15–17] The other possibility is that the pentagons and heptagons get frozen-in, effectively becoming topological defects in graphene such as pentagon-octagon defects (5–8 defects), double pentagon-heptagon pair defects [Stones-Wales (SW) defects], or triple pentagon-

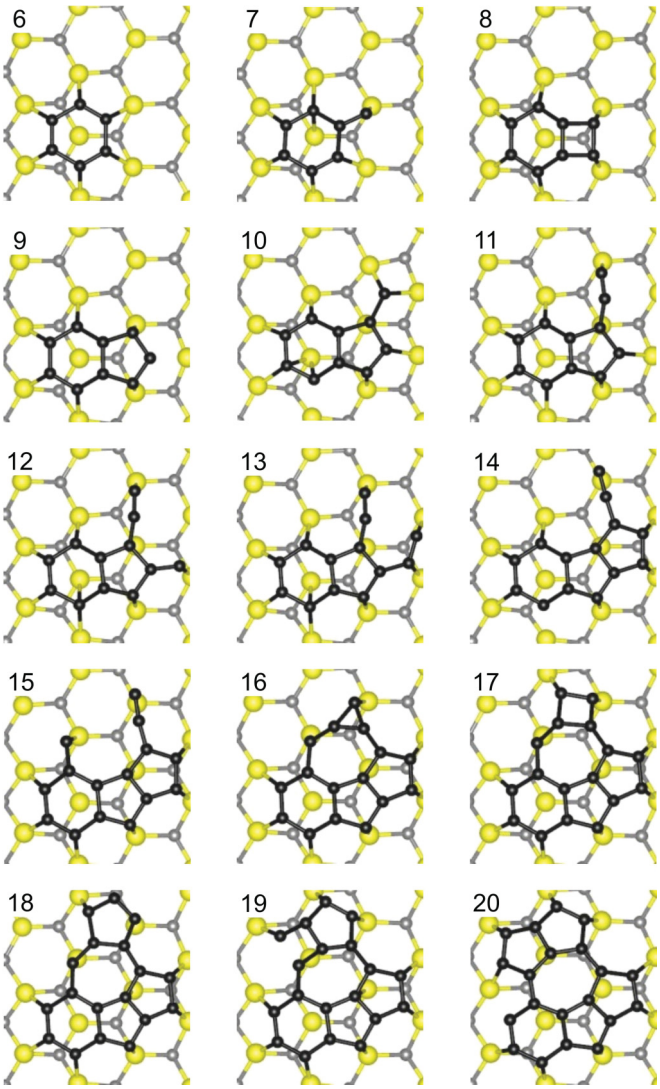

FIG. 3. (Color online) Structural evolution of a cluster during the growth of a penta-heptagonal cluster on SiC(0001). Numbers show the number of C atoms.

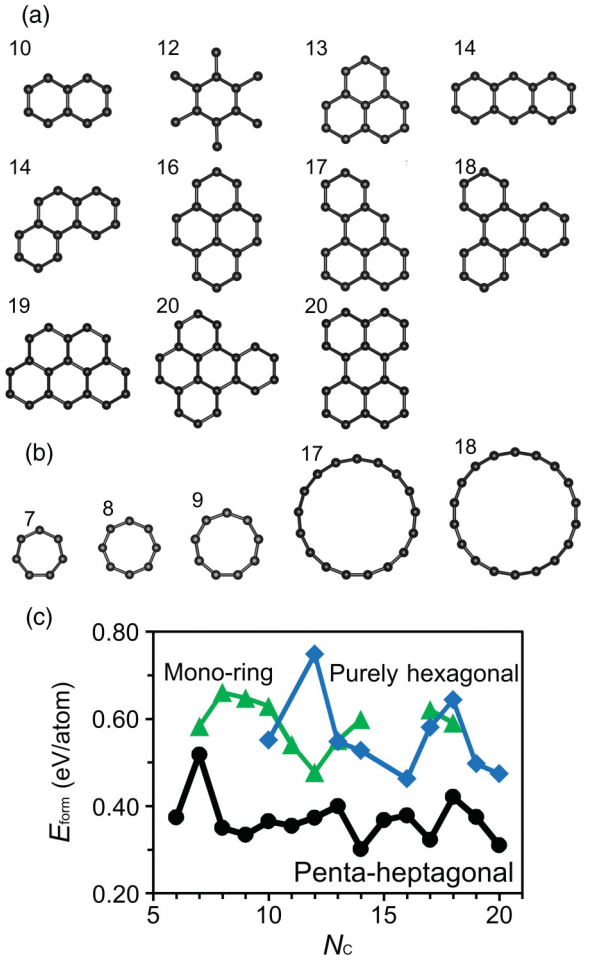

FIG. 4. (Color online) Comparison to the penta-heptagonal structure. (a) Referenced purely hexagonal. (b) Referenced mono-ring clusters. To reduce space, the C_{10-16} mono-ring clusters are omitted. (c) The formation energy of C clusters as a function of the number of C atoms N_C. Black corresponds to penta-heptagonal clusters. Also shown are the formation energies of purely hexagonal (blue/medium gray) and mono-ring (green/light gray) clusters for their lowest-energy configuration.

heptagon pair defects (T5T7 defects). However, the energy to induce a 5–8, SW, or T5T7 defect in free-standing graphene is 7.2, 4.9, or 6.6 eV, respectively, which reaches to the cohesive energy of graphite (7.4 eV/atom).[18] Hence, even though these defects remain in a graphene sheet, they may transform into several hexagons; that is, they may become a perfect graphene (purely hexagonal) structure after thermal annealing process.

B. Bonding state of C clusters on SiC(0001)

Energetics of C clusters is strongly affected by chemical bonds in and/or around clusters. Here, we focus on bonding state of penta-heptagonal clusters on SiC(0001). Macroscopically, the formation energy of a 2D penta-heptagonal island is described by the bulk energy term and the edge energy term, for this case being $E_{\text{form}} = \mu_{\text{grn/SiC}} + \gamma/\sqrt{N_C}$. Here $\mu_{\text{grn/SiC}}$ is the chemical potential of C atoms in graphene on SiC(0001), which depends on interfacial bonds between the penta-heptagonal structure and SiC(0001) and lateral strain of graphene, γ is the edge energy per atom, and $\sqrt{N_C}$ is proportional to the edge length L. This formula suggests that the formation energy E_{form} asymptotically decreases to the chemical potential $\mu_{\text{grn/SiC}}$ as N_C increases. However, even though E_{form} shows large energy drops of -0.1 eV/atom, the formation energy in Fig. 4(c) does not show the asymptotical decrease, remaining near its average 0.37 eV/atom. The energy drops are due to the formation of C-C bonds corresponding to the emergence of new tetragonal or pentagonal rings in Fig. 3. But the constant average value of the formation energy suggests that all atoms in the clusters have the same edge energy. This result is consistent with the small cluster sizes, in which every atom is an edge atom. Therefore, the formation energy may be written as a constant value: $E_{\text{form}} = \mu_{\text{grn/SiC}} + \gamma$. It has been known that $\mu_{\text{grn/SiC}}$ of the SiC(0001)-$(\sqrt{3} \times \sqrt{3})$R30° structure is -0.26 eV/atom.[9,19] Using this value, γ equals 0.63 eV/atom, which is much less than 5.68 eV/atom, the edge energy of free-standing purely hexagonal or that of a wide graphene nanoribbon with the lowest-energy reconstruction edge (a reconstruction

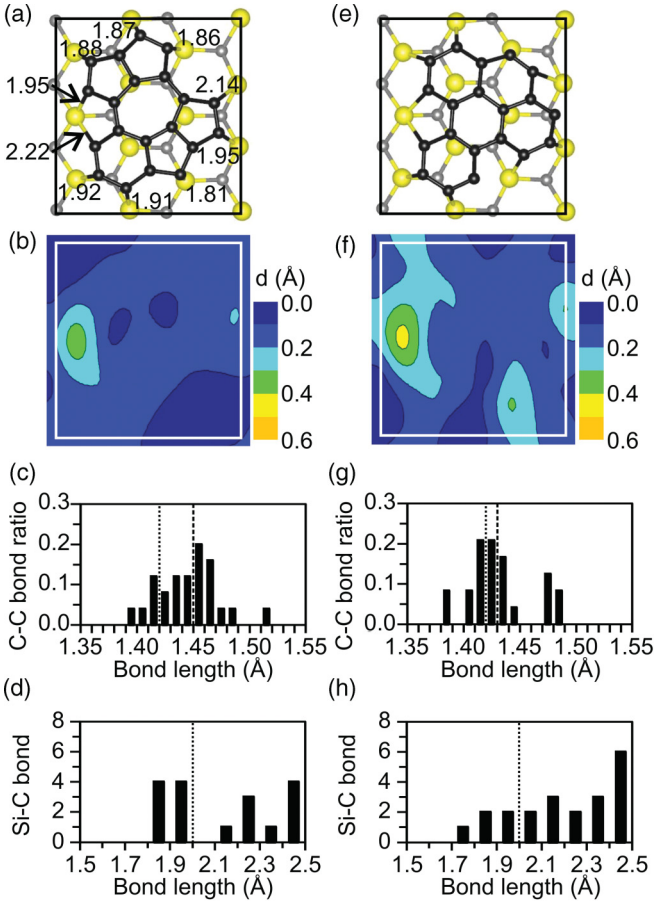

FIG. 5. (Color online) Structural analysis of the penta-heptagonal and purely hexagonal C_{20}. (a) Atomic configuration of the penta-heptagonal C_{20}. Numbers are Si-C bond lengths between the edge of the cluster and SiC(0001). (b) Distribution of displacements of each atom in the top bilayer of SiC(0001) under the penta-heptagonal C_{20}. The solid square corresponds to that in (a). The origin of the distribution is a relaxed bare SiC(0001). (c) Distribution of C-C bond lengths in the penta-heptagonal C_{20}. Number of bonds is normalized by the total number of C-C bonds. Dashed line shows the average in the cluster. Dotted line is C-C bond length of free-standing graphene. (d) Distribution of number of Si-C bond lengths between the penta-heptagonal C_{20} and SiC(0001). (e)–(h) Those of the purely hexagonal cluster C_{20}.

of a zigzag edge in which two hexagons transform into a pentagon and a heptagon) at 2.36 eV/atom.[15,20] This result implies that dangling bonds at the edge of penta-heptagonal C clusters terminate by forming Si-C bonds with SiC(0001). In fact, each C atom at the edge of the C cluster C_{20} have nonpassivated Si atoms on SiC(0001) within a distance of 1.81 to 2.22 Å [Fig. 5(a)]. This range covers the bond length of the first-nearest-neighbor Si-C bonding in bulk SiC (2.02 Å), implying the formation of Si-C bonds.

In addition to this edge bonding, Fig. 5(d) suggests that the penta-heptagonal C_{20} on SiC(0001) have out-of-plane interfacial bonds with SiC(0001), as theoretically revealed for the SiC(0001)-$(6\sqrt{3}\times 6\sqrt{3})$R30° structure. The SiC(0001)-$(6\sqrt{3}\times 6\sqrt{3})$R30° structure is stabilized by the interfacial bonds and a lack of lattice mismatch.[21] On the other hand, small C clusters, which cannot undergo large-scale reconstruction, may stabilize by forming more first-nearest-neighbor bonds with SiC(0001), in which the C atom in the cluster and the Si atom just under that form Si-C bond, than the SiC(0001)-$(6\sqrt{3}\times 6\sqrt{3})$R30°. Compared to the SiC(0001)-$(6\sqrt{3}\times 6\sqrt{3})$R30° structure, the SiC(0001)-$(\sqrt{3}\times\sqrt{3})$R30° structure has denser first-nearest-neighbor bonding with SiC(0001), expanding by 8% due to the large lattice mismatch between graphene and SiC(0001). Therefore, if a small C cluster consisted of only hexagons and had dense interfacial bonding to SiC(0001), substantial interfacial strain, i.e., tensile strain in the C cluster and compressive strain in SiC(0001), would occur.

Analyzing distribution of C-C bond lengths of the penta-heptagonal C_{20} [Fig. 5(c)], we confirmed that the average C-C bond length is 1.45 Å, which is longer than that of free-standing graphene (1.42 Å). This means C-C bonds in the small cluster are expanded by 2% as the SiC(0001)-$(\sqrt{3}\times\sqrt{3})$R30° structure. Besides, displacement distribution of each atom in the top bilayer of SiC(0001) shows structural deformations from the relaxed bare surface, indicating the compressive strain [Fig. 5(b)].

We can summarize the bonding state of C clusters on SiC(0001). C clusters form the edge and interfacial bonding with SiC(0001), while they suffer from tensile strain due to the lattice mismatch. The lattice mismatch also causes compressive strain in SiC substrate.

C. Structural analysis of penta-heptagonal and purely hexagonal clusters

Next, we discuss the energetic preference of penta-heptagonal clusters than those of purely hexagonal, because the emergence of penta-heptagonal (nonpure hexagonal) clusters was unexpected. Comparing the interfacial bonding and strain (discussed above) between penta-heptagonal clusters and those of purely hexagonal, we can understand the stability of penta-heptagonal structures. Here, we analyze the penta-heptagonal [Fig. 5(a)] and purely hexagonal [Fig. 5(e)] C_{20}, carefully.

At first, we investigate the interfacial strain. Figures 5(c) and 5(g) show distribution of C-C bond lengths in the penta-heptagonal and purely hexagonal C_{20} on SiC(0001). The average C-C bond lengths of the penta-heptagonal and purely hexagonal are 1.45 and 1.43 Å (tensile strain of 2 and 1%), respectively. Although the difference of tensile strain is slight, we can recognize that structural deformations in SiC(0001) for the purely hexagonal is clearly larger than that of the penta-heptagonal [Figs. 5(b) and 5(f)]. Results also suggest that the effect of the interfacial strain is mainly due to strain in the substrate, because the structural disorder induced in the substrate is about 0.1 Å, while that in C cluster is 0.01 Å. Therefore, it is implied that the penta-heptagonal structure can lessen the interfacial strain.

In addition, distance distribution between C atoms in the penta-heptagonal C_{20} and Si atoms in SiC(0001) exhibits a sharp peak within a range of 1.8 to 2.0 Å [Fig. 5(d)], while this peak broadens for the purely hexagonal C_{20} [Fig. 5(h)]. This indicates that the penta-heptagonal structure can make more appropriate Si-C bonds (corresponding to the first-nearest-neighbor bonding of SiC crystal) with SiC(0001).

We conclude that the small C clusters should form a penta-heptagonal structure, avoiding critical interfacial tensile strain and making more appropriate bonds with SiC(0001). Pentagons and heptagon in the penta-heptagonal C_{20} adjust its lattice and reduce the lattice mismatch. Indeed, some hexagons in the purely hexagonal transformed into pentagons during atomic structure optimizations to increase the interfacial bonds and reduce the strain.

D. Comparison with the lowest-energy free-standing C clusters

The preference of small C clusters on SiC(0001) for the penta-heptagonal structure contrasts to that of C clusters without SiC(0001) and under vacuum (i.e., free-standing C clusters). The lowest-energy structure of free-standing, small C clusters is linear for C_{2-5}, mono-ring for C_{6-18}, and penta-heptagonal for C clusters larger than C_{19}, respectively.[20,22] But how much does the non-penta-heptagonal mono-ring structure stabilize C clusters on SiC(0001)? To answer this question, we compared the energetic stability of the mono-ring clusters in Fig. 4(b) with that of the penta-heptagonal clusters on SiC(0001).

The formation energy of the most stable configuration of C mono-ring clusters exceeds those of penta-heptagonal structures by 0.1–0.3 eV [Fig. 4(c)]. Moreover, some of the initial configurations, including all C_{15} and C_{16} clusters, did not retain their original configuration through the optimization procedure, transforming into a penta-heptagonal structure or decomposing into smaller linear clusters. These results indicate that penta-heptagonal clusters on SiC(0001) have lower energy than C clusters with the mono-ring structure. In other words, SiC(0001) acts as an atomic template for the growth of graphene.

The energetic stability of free-standing C mono-ring clusters originally arises from C-C multiple bonds. However, on SiC(0001), formation of Si-C bonds between C cluster and SiC(0001) modulates these C-C bonds. This can be confirmed from Fig. 6. After the structure optimization, the mono-ring structure C_{18} was strongly deformed [Fig. 6(a)]. The mono-ring cluster C_{18} has a wide range of C-C bond length, including single (1.42 Å) and double (1.33 Å) C-C bonding [Fig. 6(b)]. Especially, all single-like C-C bonds (bond length between 1.39 and 1.51 Å) in the cluster are made between C atoms binding with Si atom on SiC(0001), as shown in Fig. 6(a). Therefore, the bonding modulation by SiC(0001) influences the multiple bonding in mono-ring clusters, the origin of the stability. In addition, degeneration of multiple bonds in mono-ring clusters may cause dangling bonds, making the cluster unstable. Although formation of Si-C bonds basically stabilize mono-ring clusters, the ground-state configuration on SiC(0001) is no longer the mono-ring structure but the penta-heptagonal one.

If the edge of free-standing C cluster is passivated by H atoms, C clusters do not have the mono-ring structure, instead having the purely hexagonal structure.[20] H passivation has the same effect with the formation of Si-C edge bonding between the penta-heptagonal cluster and SiC(0001), neglecting the interfacial strain. By considering the formation of Si-C bonds between the edge of a C cluster and SiC(0001), we conclude that SiC(0001) promotes the formation of the penta-heptagonal structure by bonding to the cluster's edge atoms.

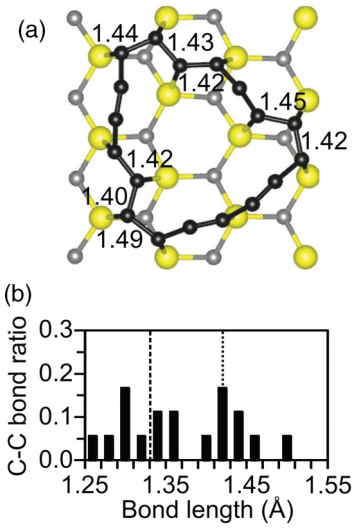

FIG. 6. (Color online) C mono-ring cluster C_{18} on SiC(0001). (a) The relaxed structure of C_{18}. Numbers are single-like C-C bond lengths in the cluster (Å). (b) Distribution of C-C bond lengths in the cluster. Dashed and dotted lines show double and single C-C bond length, respectively.

E. Trigger of C clustering

Although above discussions have revealed the lowest-energy structures of C clusters and their energetics, clarification of a trigger of C clustering is essential for control of the nucleation rate. If the chemical potential of monatomic C migrating on SiC(0001) exceeds that of C clusters, C atoms will begin to aggregate. So, we now analyze the chemical potential of C atoms on SiC(0001). Assume that the chemical potential depends on the temperature and the surface coverage of monatomic C as $\mu_{\mathrm{mono}} = E_{\mathrm{form/mono}} - k_{\mathrm{B}}T \ln N_s$.[23] Here, $E_{\mathrm{form/mono}}$ is the formation energy of a C monomer on SiC(0001), k_{B} is the Boltzmann constant, T is the temperature, and N_s is the number of adsorption sites on SiC(0001). These sites are the T4 and H3 sites, which are determined by the C-monomer coverage. To compute the formation energy of a C monomer, we assumed that the monomers occupy T4 sites, and then we minimized the dangling bonds of Si atoms on SiC(0001) for each coverage value.

Figure 7(a) shows four coverage θ values [0.17 to 0.42 atom/SiC(0001)-(1 × 1)] at the initial stage before clustering. For these four values, we obtained the chemical potential at 0, 1000, and 2000 K. The results are in Fig. 7(c). Comparing the chemical potential at $T = 0$ K to that at other temperatures ($T = 1000$, 2000 K), we found that the enthalpy term dominates the chemical potential and the enthalpy drastically increases as the coverage increases.

For the coverage between 0.17 and 0.33 atom/SiC(0001)-(1 × 1), the number of dangling bonds on the surface certainly decreases due to C adsorption. However, the formation energy does not decrease but rather increase. To understand the increase of the enthalpy, we examined strain in SiC(0001) induced by C adsorption. As shown in Fig. 7(b), it was found

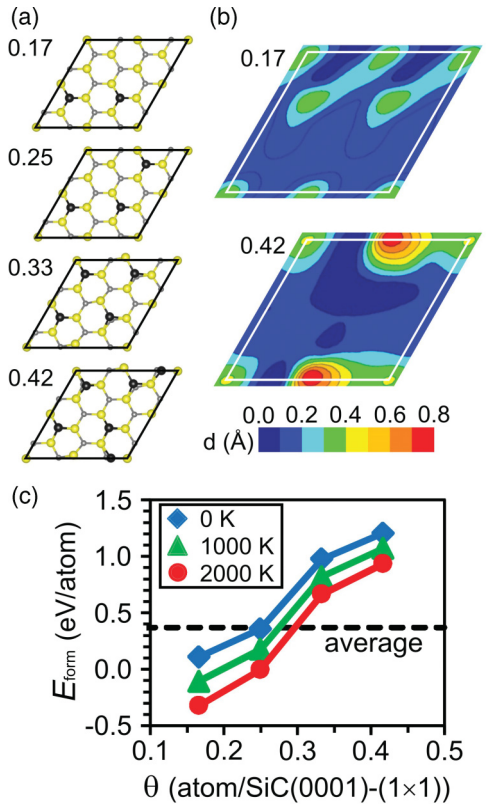

FIG. 7. (Color online) Calculation of the chemical potential of monatomic C migrating on SiC(0001). (a) Surface model for C-adsorbed SiC(0001) lateral unit cell. Numbers are the surface coverage of C atoms, which are shown as thick black circles. (b) Distribution of displacements of each atom in the top bilayer of SiC(0001) for the coverage of 0.17 and 0.42 atom/SiC(0001)-(1 × 1). The origin of the distribution is a relaxed bare SiC(0001). Numbers are the surface coverage of C atoms. The region enclosed by solid lines is corresponding to the surface shown in (a). (c) The chemical potential of C atoms as a function of the coverage and the temperature. The dashed line marks the average formation energy of the most stable C clusters on SiC(0001).

that a C monomer cause structural disorder in SiC(0001) and the disorder is enhanced by adding more monomers. Therefore, the enthalpy increases because of the strain.

According to the results in Fig. 7(c), the coverage at which the chemical potential of monatomic C exceeds the average formation energy of C clusters equals 0.25–0.33 atom/SiC(0001)-(1 × 1). Above this value, C clusters on SiC(0001) become more energetically stable than the environment suffering from the strain, and thus C atoms should begin clustering. Therefore, the trigger for C clustering on SiC(0001) is the increase of the enthalpy term, which occurs with an increase of surface strain. Then, when C clusters on SiC(0001) become large enough to decrease their formation energies, the driving force for growth increases, thus accelerating the rate of growth.

IV. CONCLUSION

In summary, we used a first-principles approach to investigate C-atom clustering on SiC(0001). A cluster was started with a C hexagon ring in the lowest-energy position and subsequently grew by developing a heptagonal ring surrounded by pentagonal rings, a penta-heptagonal structure. The clustering process begins due to an increase of the enthalpy term in the chemical potential of the C atoms. The enthalpy term drastically increases with increasing C coverage, and at the coverage of 0.25–0.33, the chemical potential of the C atoms exceeds that of the C clusters. Our first-principles study has revealed the structural evolution of small C clusters in the initial stage of 0^{th}-layer graphene growth and shown that SiC(0001) can act as a graphene template for clustering C atoms.

ACKNOWLEDGMENTS

This work was partially supported by a Grant-in-Aid for JSPS Fellows (40-7700). One of the authors (M. Inoue) acknowledges the partial support by Innovation Training Program Center for R&D and Business Leaders of Kyushu University.

*Corresponding author: minoue@riam.kyushu-u.ac.jp

[1] A. J. Van Bommel, J. E. Crombeen, and A. Van Tooren, Surf. Sci. **48**, 463 (1975).
[2] J. Hass, R. Feng, T. Li, X. Li, Z. Zong, W. A. de Heer, P. N. First, E. H. Conrad, C. A. Jeffrey, and C. Berger, Appl. Phys. Lett. **89**, 143106 (2006).
[3] H. Hibino, H. Kageshima, F. Maeda, M. Nagase, Y. Kobayashi, and H. Yamaguchi, Phys. Rev. B **77**, 075413 (2008).
[4] S. H. Ji, J. B. Hannon, R. M. Tromp, V. Perebeinos, J. Tersoff, and F. M. Moss, Nat. Mater. **11**, 114 (2012).
[5] J. B. Hannon and R. M. Tromp, Phys. Rev. B **77**, 241404(R) (2008).
[6] S. Tanaka, K. Morita, and H. Hibino, Phys. Rev. B **81**, 041406(R) (2010).
[7] W. Norimatsu and M. Kusunoki, Physica E **42**, 691 (2010).
[8] T. Ohta, N. C. Bartelt, S. Nie, K. Thurmer, and G. L. Kellogg, Phys. Rev. B **81**, 121411(R) (2010).
[9] H. Kageshima, H. Hibino, M. Nagase, and H. Yamaguchi, Appl. Phys. Express **2**, 065502 (2009).
[10] M. Inoue, Y. Kangawa, K. Wakabayashi, H. Kageshima, and K. Kakimoto, Jpn. J. Appl. Phys. **50**, 038003 (2011).
[11] K. V. Emtsev, A. Bostwick, K. Horn, J. Jobst, G. L. Kellogg, L. Ley, J. L. McChesney, T. Ohta, S. A. Reshanov, J. Röhrl, E. Rotenberg, A. K. Schmid, D. Waldmann, H. B. Weber, and T. Seyller, Nat. Mater. **8**, 203 (2009).
[12] R. M. Tromp and J. B. Hannon, Phys. Rev. Lett. **102**, 106104 (2009).
[13] J. P. Perdew, K. Burke, and M. Ernzerhof, Phys. Rev. Lett. **77**, 3865 (1996).
[14] R. O. Jones, J. Chem. Phys. **110**, 5189 (1999).
[15] P. Koskinen, S. Malola, and H. Hakkinen, Phys. Rev. Lett. **101**, 115502 (2008).
[16] Ç. Ö. Girit, J. C. Meyer, R. Erni, M. D. Rossell, C. Kisielowski, L. Yang, C.-H. Park, M. F. Crommie, M. L. Cohen, S. G. Louie, and A. Zettl, Science **323**, 1705 (2009).

[17] P. Koskinen, S. Malola, and H. Hakkinen, Phys. Rev. B **80**, 073401 (2009).
[18] E. Cockayne, Phys. Rev. B **85**, 125409 (2012).
[19] A. Mattausch and O. Pankratov, Phys. Rev. Lett. **99**, 076802 (2007).
[20] D. P. Kosimov, A. A. Dzhurakhalov, and F. M. Peeters, Phys. Rev. B **81**, 195414 (2010).
[21] S. Kim, J. Ihm, H. J. Choi, and Y. W. Son, Phys. Rev. Lett. **100**, 176802 (2008).
[22] D. P. Kosimov, A. A. Dzhurakhalov, and F. M. Peeters, Phys. Rev. B **78**, 235433 (2008).
[23] H. Kageshima, A. Taguchi, and K. Wada, J. Appl. Phys. **100**, 113513 (2006).